Two way relationship between aerosols and fog: A case study at IGI Airport, New Delhi

Pramod Digambar Safai[1*], Sachin Ghude[1], Prakash Pithani[1], Somnath Varpe[1], Rachana Kulkarni[1], Kiran Todekar[1], Suresh Tiwari[1], Dilip Motiram Chate[1], Thara Prabhakaran[1], Rajendra Kumar Jenamani[2] and Madhavan Nair Rajeevan[3]

1. Indian Institute of Tropical Meteorology, Pune, 2. India Meteorological Department, New Delhi, 3. Ministry of Earth Sciences, New Delhi

Corresponding Author: pdsafai@tropmet.res.in

Abstract

The frequency and intensity of fog episodes during the winter season has been increasing during the past decade over the mega city of Delhi due to the high pollution load. The role of atmospheric aerosols is very important in the life cycle of fog in the urban areas. This paper presents the results on variation of aerosol optical properties (scattering and absorption coefficients) and black carbon (BC) mass concentration during the foggy period in winter season (December 2015 to February 2016) at the Indira Gandhi International (IGI) Airport, New Delhi. The interaction between scattering and absorbing aerosols and fog before, during and after the foggy period has been studied for a typical case. BC mass concentration along with aerosol scattering and absorption coefficients showed enhancement before and during the initial phase of dense foggy period. However, there was a steep decrease in them after the sustenance of dense fog which infers towards their possible scavenging by fog droplets. Also, it was observed that the decrease in ambient temperature and depression temperature (DT); and increase in relative humidity (RH) played a major role in sustenance of dense fog inspite of reduction in aerosol load. Single scattering albedo (SSA) showed decrease during dense fog due to comparatively more reduction in scattering aerosols than absorbing type. Both scattering and absorption coefficients showed significant correlation with cloud condensation nuclei (CCN).

Keywords: New Delhi Airport, Winter fog, Scattering and absorption coefficients, Black carbon, Visibility.

1. Introduction

Fog is comprised of visible cloud water droplets or ice crystals suspended in the air at or near the surface of the earth (Gultepe, 2007). Fog is influenced by nearby water bodies, topography of the region, prevailing winds and availability of aerosols suspended in the air which are originated from different natural sources and man-made activities. Heavy and persistent fog is a common feature in the winter season over the northern Indian region and it is one of the major weather disasters that impacts all forms of transport including aviation, rail and road journey. Cosequently it affects the human activities, economy and overall life of the people in the region. Maximum occurrence of fog over northwest India is about 48 days every year with atmospheric visibility < 1000 m, mostly during the months of December to February. Over the Indo Gangetic Plains (IGP) region, the frequency of fog occurrence has significantly increased during winter months in the last four decades (Srivastava, et al, 2016). In spite of its regular occurrence and impotance in various human related phenomena, we still lack the understanding of the physical and chemical characteristics of fog and reasons for its rapid thickening over the IGP region. In addition, the information on role of meteorological factors responsible for formation, sustenance and dissipation of fog is required for sufficiently reliable forecast of fog and thereby proper and timely mitigation of the fog events. Therefore, an intensive ground-based measurement campaign termed as Winter fog experiment (WIFEX) was conducted at the ~~Indira Gandhi International Airport (~~IGI Airport ~~)~~, New Delhi under the the initiation by Ministry of Earth Sciences, Government of India. Extensive set of comprehensive ground based instrumentation for observations on surface ~~micro~~meteorological parameters, radiation balance, turbulence, thermodynamical structure of the surface layer, fog droplet and aerosol microphysics, aerosol optical properties, and aerosol and fog water chemistry were deployed at the IGI Airport (Ghude et al., 2017).

Several studies have underlined the importance of aerosols in fog life cycle over the IGP region (Ganguly et al., 2006; Gautam et al., 2007; Das et al., 2008; Safai et al., 2008; Mehta et al., 2009; Mohan and Payra, 2014; Tripathi et a., 2006). However, there is a need for understanding the interaction of aerosols with fog microphysical processes. Growth of fog droplets depends on the physicochemical properties of the aerosols. Hygroscopic aerosols which act as CCN, can influence fog supersaturation and its formation. Several studies have been reported concerning the aerosol-fog interaction (Cheng and Tsai, 2000; Elias et al., 2009; Singh and Dey, 2012; Zhao et al., 2016; Liu et al., 2016; Molnar et al., 2016; Chen et al., 2016; Chelani, 2017). In the present paper, results related with variation of aerosol scattering and absorption coefficients, mass concentration of ~~black carbon (~~BC~~)~~ aerosols during the dense foggy conditions as well as before its commencement and during the dissipation stage are discussed. The changes in meteorological parameters such as temperature, relative humidity ~~(RH)~~ and atmospheric pressure are also studied. The results obtained from this study will be useful in the on going research in aerosol-fog interaction and subsequent mitigation strategies aimed towards controlling the adverse impacts of poor atmospheric visibility conditions faced by the entire northern Indian region during the winter months.

2. Sampling Location and Methodology

The observations were carried out at about 15 m above the ground at IGI Airport, New Delhi ($28^0.56^{'}$ N, $77^0.09^{'}$ E) during December 2015 to February 2016. At the airport, there is a vast open area experiencing frequent fog formation particularly during the winter season and observations of visibility are routinely carried out over there. Instruments were installed on the northern side of the airport which is about 400 m away from the runway that was less operational during the WIFEX observational period. Aerosol scattering coefficient (σ_{sca}) was measured using a multi wavelength integrating nephelometer (Aurora 3000, Ecotech, Australia) at one minute interval. An aethalometer (AE-33/7, Magee Sci, USA) was used to measure BC mass at one

minute interval. In addition to the BC mass, this equipment also shows the percentage fraction of BC from biomass burning using the method applied by Sandradewi et al (2008a, 2008b). The next generation aethalometer also gives the corrected BC mass concentration after applying dual spot technique to compensate for the filter loading effect thereby reducing the uncertainty in the measurements (Drinovec et al, 2015). The BC mass was further used to compute the absorption coefficient (σ_{abs}). Absorption and scattering coefficients at a common wavelength 520 nm were considered in this study for comparison and computation of extinction coefficients and single scattering albedo (SSA).

Observations on visibility were obtained from India Meteorological Department (IMD) through their run way visual range (RVR) systems installed along the run way at IGI Airport. Also, simultaneous observations on meteorological parameters (temperature, relative humidity ~~(RH),~~ and atmospheric pressure) were carried out during the study period. In addition, observations on cloud condensation nuclei ~~(CCN)~~ were carried out using CCN Counter (Droplet Measurement Technologies, USA). Details on these observations are mentioned elsewhere (Ghude et al., 2017).

3. Results and Discussion

3.1 Variation of BC mass and aerosol optical properties during fog

Atmospheric BC aerosols mainly originate from incomplete combustion processes involving fossil fuel and biomass burning activities. Fig.1a depicts the daily mean mass concentration of BC in comparison with the atmospheric visibility at IGI Airport during the study period. The BC concentration varied from 8.0 to 58.3 μgm^{-3} during the entire period with mean concentration of 18.2 ± 8.3 μgm^{-3}. It was observed on many occasions that BC concentration showed enhancement prior to the very dense fog (visibility < 50 m). Dey et al (2006) have reported BC mass concentration of 15 μgm^{-3} during clear days which increased to 65 μgm^{-3}

during foggy/hazy days at Delhi during the winter season of 2004. Smoke and absorbing aerosols were reported to be the major constituents of winter fog over Pakistan (Khokhar et al, 2016). Similarly Safai et al (2008), Niranjan et al (2007) and Ramachandran et al (2006) have reported increase in BC mass during winter fog at Agra, Kharagpur and Hisar, respectively. BC correlated negatively with visibility ($r = - 0.51$, $p < 0.0006$). As observed from Fig. 1b, both σ_{sca} and σ_{abs} showed increase during foggy days indicating impact of scattering as well as absorbing aerosols on fog formation. During the entire observational period, the mean σ_{sca} was 403 ± 263 Mm^{-1} which varied from 99 to 1316 Mm^{-1} whereas; the mean σ_{abs} was 251 ± 102 Mm^{-1} which varied from 111 to 485 Mm^{-1}. There was a negative correlation between σ_{sca} and visibility ($r = - 0.35$, $p < 0.03$) and similarly between σ_{abs} and visibility ($r = - 0.48$, $p < 0.006$). This indicates towards important role of atmospheric aerosols in the visibility degradation particularly during the winter months over this region. The biomass burning percentage (BB %) to total BC mass can be obtained from inbuilt software of the aethalometer AE33 using the Sandradewi model (~~Aethalometer Model AE33 User Manual, 2014~~ Sandradewi et al, 2008b). BB % to BC mass was ~~also~~ studied for this period. The mean BB% to total BC mass was 12.8 ± 5.4 % with values varying between 1 to 24 %. This indicates towards dominance of fossil fuel burning at the observational site mainly due to the aviation related activities at the airport.

Reduction in atmospheric visibility is related with the attenuation of light ~~either~~ from gases ~~or~~ and aerosols. In the present study, we are considering light attenuation due to aerosols only. Light attenuation by aerosols is through scattering and absorption and is represented by extinction coefficient (σ_{ext}) which is obtained by addition of σ_{sca} and σ_{abs}. Using the σ_{sca} and σ_{abs} data; σ_{ext} has been computed and further an attempt is made to calculate the atmospheric visibility by applying Koschmieder formula on relationship between visibility and σ_{ext} (Hovrath, 1971) as follows (Eq.1):

$$\text{Visibility} = 3.219 / \sigma_{ext} \quad \text{----------} \quad (1)$$

The number 3.912 denotes the minimum observable contrast between an appropriately large, black object against the horizon sky called the contrast threshold.

It was observed that the visibility as computed from this method compared reasonably well with that measured by RVR at the airport (Fig. 2). The computed and measured visibility correlated well with each other ($r = 0.60$, $p < 0.0003$). This indicates towards the vital role of aerosols in the visibility degradation and thereby in the mechanism of fog formation.

3.2 A typical case study on variation of aerosols during dense foggy period

In the present study, a typical data set on dense foggy period (visibility < 1000 m) during 2100 hr IST on 23 Jan 2016 to 0500 hr IST on 24 Jan 2016 is considered in comparison with the same time duration on 16-17 Jan 2016 and 1-2 Feb 2016 as proxy for less foggy days before and after the dense fog, respectively (Fig. 3). Mean BC mass concentration was 43 μgm^{-3} that ranged from 36 to 51 μgm^{-3} during this dense foggy period. It was 13 μgm^{-3} during the less foggy period both prior to dense fog and after dense fog. Thus there was > 3 times more BC mass during dense foggy period than that during less foggy period. Both σ_{sca} and σ_{abs} at 520 nm also showed significant increase during dense foggy period as compared to the less foggy period. During the dense foggy period, the mean σ_{sca} was 757 Mm^{-1} whereas; the mean σ_{abs} was 559 Mm^{-1}. Whereas during less foggy period period prior to dense fog, mean σ_{sca} and σ_{abs} were respectively 469 and 173 Mm^{-1} and the same during less foggy period after the dense fog were respectively 309 and 174 Mm^{-1}.

Using the σ_{sca} and σ_{abs}, single scattering albedo (SSA) at 520 nm was computed for the dense foggy as well as less foggy period as (Eq.2):

$$SSA = \sigma_{sca} / (\sigma_{sca} + \sigma_{abs}) \quad (2)$$

SSA is one of the important climate variables in the aerosol radiation studies. More SSA indicates dominance of scattering aerosols that leads to cooling effect whereas, low SSA shows more

158 absorbing type aerosols leading to warming effect (Goody, 1996; Takemura et al, 2002). In the
159 present study, SSA values decreased during the dense foggy period. Mean SSA was 0.59 during
160 dense foggy period whereas it was 0.74 and 0.61 during less foggy period before and after dense
161 fog, respectively. Increase in absorbing aerosols i.e. BC was accompanied by decrease in SSA
162 during dense foggy period. Ramachandran et al (2006) have reported low SSA values during
163 foggy conditions (0.76) as compared to that in clear conditions (0.88) at Hisar; which was
164 attributed to more absorbing (BC) aerosols.

165 However during the dense fog, even though BC, σ_{sca} and σ_{abs} showed increase in the
166 initial hours; there was decrease in the latter phase with about 50 % reduction within next few
167 hours. As seen from Fig. 4 (a), mass concentration of BC which had reached up to 51 μgm^{-3}
168 during the onset and initial phase of dense fog (at around 02.45 hr on 24 Jan 2016), declined
169 gradually to reach up to about 27 μgm^{-3} at around 05.00 hr on 24 Jan 2016. Almost similar
170 trend was observed during this period for σ_{sca} and σ_{abs} (Fig. 4c and 4d) with values decreasing
171 from 900 Mm^{-1} to 350 Mm^{-1} for σ_{sca} and those for σ_{abs} reduced from 670 Mm^{-1} to 360 Mm^{-1}. This
172 clearly infers towards scavenging of both scattering and absorbing aerosols as well as hydrophilic
173 and hydrophobic aerosols and their conversion into fog droplets (Dall'Osto et al., 2009). Also, the
174 SSA decreased during dense foggy period from 0.66 to 0.45 (Fig. 4b). This is indicative of less
175 scavenging of absorbing aerosols as compared to that of scattering type. As already mentioned in
176 section 3.1, there is > 80 % contribution to BC from fossil fuel sources which could mainly be
177 hydrophobic in nature and thereby responsible for less scavenging by fog droplets.

178 The further interesting part is that even though aerosols showed steep decline after the
179 initial phase of dense fog formation; the dense fog itself persisted for several hours even reaching
180 the minimum visibility of ≤ 50 m during 04.00 to about 07.00 hr and up to 200 m till 10.30 hr on
181 24 Jan 2016. Therefore, it is quite clear that the other controlling factors mainly prevailing
182 meteorological conditions took over the responsibility of sustenance of dense fog. This is

confirmed from the data on ambient temperature, relative humidity and atmospheric pressure at the sampling site. Fig. 5 shows the variation of various meteorological parameters during this period in comparison with atmospheric visibility. It can be observed that ambient temperature decreased from 12.5^{0}C at the onset of dense fog on 24 Jan 2016 to about 8.5 ^{0}C at commencement of very dense fog with visibility < 50 m (around 02.45 hr) to as low as 6.8 ^{0}C during very dense fog at around 7 hr on 24 Jan 2016. During this period, RH also showed gradual increase from about 89 % to reach 100 % and atmospheric pressure decreased from 993.5 mb to 991.5 mb. Dew point temperature (Td) was also computed for this period as (Eq. 3):

$$Td = T - ((100 - RH) / 5) \quad (3)$$

Where T and RH represent measured ambient temperature and relative humidity, respectively. Td showed decrease from 10.5 ^{0}C to 6.8 ^{0}C during this period. During the dense foggy period, atmospheric visibility showed a significantly ~~good~~ positive correlation with temperature and Td ($r = 0.83$, $p < 0.0001$) whereas negative correlation was observed between RH and visibility ($r = -0.85$, $p < 0.0001$). Further, the depression temperature (DT) was computed as difference between T and Td (Tiwari, et al, 2011). DT showed decrease from 2.1 to 0 from the initial fog formation (visibility < 1000m) to its development in very dense fog (visibility < 50 m) and remained 0 through out the very dense foggy period till about 10.30 hr in the morning of 24 Jan 2016. All the aerosol parameters (BC, σ_{sca} and σ_{abs}) showed gradual increase from 10.30 hr on 24 Jan 2016 when dissipation of dense fog started. Thus, it is seen that even though aerosols which acted as nuclei for fog formation in the initial phase/onset, latter on got reduced due to scavenging by fog droplets. This mutual dependency indicates towards the two way relationship between aerosols and fog with aerosols playing critical role during the formation of fog and latteron fog controlling the aerosol abundance through the scavenging mechanism. The dense fog still persisted even though the aerosols decreased mainly due to the favourable meteorological conditions till its

dissipation. The important role of atmospheric temperature and RH along with the air quality including both particulate and gaseous components on observed fog trends is discussed by Klemm and Lin (2016).

It was also observed that the cloud condensation nuclei (CCN) and both σ_{sca} and σ_{abs} showed similar variation during the dense foggy period on 23-24 Jan 2016 (Fig. 6 a and b) and CCN correlated significantly well with them ($r = 0.91$, $p < 0.0001$ and $r = 0.81$, $p < 0.0001$ respectively with σ_{sca} and σ_{abs}). This indicates towards the important role of both scattering and absorbing aerosols in the formation of CCN at ground level i.e. fog droplets. Scattering aerosols are generally hygroscopic and act as good CCN. Whereas, absorbing aerosols (BC) are not considered as good CCN. Especially, the freshly emitted BC particles are reported to be hydrophobic in nature (Zhang et al, 2008). However, when they are aged or when they come into contact with other hygroscopic aerosols, their morphological and chemical properties get changed and they can act as CCN (Dusek *et al*., 2006; Furutani et al., 2008). Maskey et al (2017) have reported activation of CCN by BC particles coated with sulphuric acid.

4. Conclusions

Observations on BC and aerosol scattering and absorption coefficients were undertaken during December 2015 to February 2016 under the winter fog campaign at the IGI Airport, New Delhi. Mass concentration of BC and σ_{sca} and σ_{abs} showed significant enhancement on foggy days. However, the micro-analysis of these parameters indicated that formation of fog could have been catalysed by enhanced load of scattering and absorbing aerosols which subsequently got reduced due to scavenging by fog droplets thereby reducing these aerosols even though the density of fog persisted mainly due to prevailing meteorological conditions such as low temperature, high RH, low atmospheric pressure and lowest depression temperature. Thus, aerosols and fog displayed a mutually dependant two way relationship with each other. Decrease in SSA during dense fog infers towards comparatively less scavenging of BC aerosols signifying fossil fuel burning as

their major source. Also, both σ_{sca} and σ_{abs} correlated significantly well with CCN indicating to the vital role of both scattering as well as absorbing aerosols in the formation of fog droplets.

Acknowledgements

Authors are thankful to the Director of IITM for his support and encouragement during the entire WIFEX Campaign. Thanks are also due to the Ministry of Earth Sciences (MoES), Government of India. Authors are grateful to all the team members of WIFEX. We thank the India Meteorological Department (IMD) for their valuable help in conducting these observations and providing meteorological and RVR data at the IGI Airport, New Delhi. Special thanks to the Grandhi Mallikarjuna Rao (G.M.R.) group and Airports Authority of India (AAI) for providing logistic support and cooperation to conduct the experiment inside IGI Airport, New Delhi.

References

Aethalometer® Model AE33 User Manual, Version 1.42, Aerosol d.o.o., Ljubljana, Slovenia, 2014.

Chelani, A.B. (2017). Study of Local and Regional Influence on PM2.5 Concentration during Odd-Even Rule in Delhi Using Causal Analysis. Aerosol Air Quality Res., 17: 1190–1203.

Chen, W., Wang, X., Zhou, S., Cohen, J.B., Zhang, J., Wang, Y., Chang, M., Zeng, Y., Liu, Y., Ling, Z., Liang, G., Qiu, X. (2016). Chemical Composition of PM2.5 and its Impact on Visibility in Guangzhou, Southern China. Aerosol Air Quality Res., 16: 2349–2361.

Cheng, M.T. and Tsai, Y.I. (2000). Characterization of visibility and atmospheric aerosols in urban, suburban, and remote areas. Sci. Total Environ. 263: 101–114.

Dall'Osto, M., Harrison, R.M., Coe, H. and Williams, P. (2009). Real-time secondary aerosol formation during a fog event in London. Atmos. Chem. Phys., 9, 2459–2469.

Das, S.K., Jayaraman, A., Misra, A. (2008). Fog-induced variations in aerosol optical and physical properties over the Indo-Gangetic Basin and impact to aerosol radiative forcing. Ann. Geophys., 26, 1345–1354, 2008.

Dey, S., Tripathi, S. N., Singh, R. P. and Holben, B. N. (2006), Retrieval of black carbon and specific absorption over Kanpur city, northern India during 2001– 2003 using AERONET data, Atmos. Environ., 40, 445–456.

Drinovec, L., Mo˘cnik, G., Zotter, P., Prévôt, A. S. H., Ruckstuhl, C., Coz, E., Rupakheti, M., Sciare, J., Müller, T., Wiedensohler, A. and Hansen. A. D. A., (2015). The "dual-spot" Aethalometer: an improved measurement of aerosol black carbon with real-time loading compensation. Atmos. Meas. Tech., 8, 1965–1979, 2015. Doi: 10.5194/amt-8-1965-2015.

Dusek, U., Reischl, G. and Hitzenberger, R. (2006). CCN activation of pure and coated carbon black particles. Environ. Sci. Technol. 40, 1223–1230.

Elias, T., Haeffelin, M., Drobinski, P., Gomes, L., Rangognio, J., Bergot, T., Chazette, P., Raut, J.C. and Colomb, M. (2009). Particulate contribution to extinction of visible radiation: Pollution, haze, and fog. Atmos. Res. 92: 443–454.

Furutani. H., Dall'Osto, M., Roberts, G. C., and Prather, K. A. (2008). Assessment of the relative importance of atmospheric aging on CCN activity derived from field observations, Atmos. Environ., 42, 3130–3142.

Ganguly, D., Jayaraman, A., Rajesh, T.A. and Gadhavi, H. (2006). Wintertime aerosol properties during foggy and no foggy days over urban center Delhi and their implications for shortwave radiative forcing. J. Geophys. Res., 111, D15217, doi: 10.1029/2005JD007029.

Gautam, R., Hsu, N.C., Kafatos, M. and Tsay, S.C. (2007). Influences of winter haze on fog/low cloud over the Indo-Gangetic plains., J. Geophys. Res. 112, D05207, doi: 10.1029/2005JD007036.

Ghude, S.D., Bhat, G. S., Prabhakaran, T., Jenamani, R.K., Chate, D.M., Safai, P.D., et al., (2017). Winter fog experiment over the Indo-Gangetic plains of India. Current Sc. 112 (4), 767-784.

Goody, R. M. (1996). Principles of Atmospheric Physics and Chemistry. Oxford University Press, NY.

Gultepe, I., Tardif, R.,Michaelides, S. C., Cermak, J., Bott, A., Bendix, J., Muller, M., Pagowski, M., Hansen, B., Ellrod, G., Jacobs, W., Toth, G., Cober, S. G. (2007). Fog research: a review of past achievements and future perspectives. Pure Appl Geophys, 164, 1121–1159.

Horvath, H. (1971). On the applicability of the Koschmieder visibility formula. Atmos. Environ., **5**, 177–184.

Khokhar, M.F., Yasmin, N., Chistie, F. and Shahid, I., (2016). Temporal Variability and Characterization of Aerosols across the Pakistan Region during the Winter Fog Periods. Atmosphere 2016, 7, 67; doi: 10.3390/atmos7050067.

Klemm, O and Huei, N. (2016). Lin. What Causes Observed Fog Trends: Air Quality or Climate Change? Aerosol Air Quality Res., 16: 1131–1142.

Liu, T., Zhuang, G., Huang, K., Lin, J., Wang, Q., Deng, C. and Fu, J.S. (2016). A Typical Formation Mechanism of Heavy Haze-Fog Induced by Coal Combustion in an Inland City in North-Western China. Aerosol Air Quality Res., 17: 98–107.

Maskey, S., Chong, K.Y., Seo, A., Park, M., Lee, K. and Park, K. (2017). Cloud Condensation Nuclei Activation of Internally Mixed Black Carbon Particles.. Aerosol Air Quality Res., 17: 867–877.

Mehta, B., Venkataraman, C., Bhushan, M. and Tripathi, S. N. (2009). Identification of sources affecting fog formation using receptor modeling approaches and inventory estimates of sectoral emissions. Atmos. Environ. 43, 1288–1295.

Mohan, M., Payra, S. (2014). Aerosol Number Concentrations and Visibility during Dense Fog over a Subtropical Urban Site. Journal of Nanomaterials, Article ID 495457. http://dx.doi.org/10.1155/2014/495457.

Molnár, A., Bécsi, Z., Imre, K., Gácser, V. and Ferenczi, Z. (2016). Characterization of Background Aerosol Properties during a Wintertime Smog Episode. Aerosol Air Quality Research, 16: 1793–1804.

Niranjan, K., Sreekanth, V., Madhavan, B.L. and Moorthy, K.K. (2007). Aerosol physical properties and Radiative forcing at the outflow region from the Indo-Gangetic plains during typical clear and hazy periods of wintertime. J. Geophys. Res. 34, L19805, doi: 10.1029/2007GL031224.

Ramachandran, S., R. Rengarajan, A. Jayaraman, M. M. Sarin, and S. K. Das (2006), Aerosol radiative forcing during clear, hazy, and foggy conditions over a continental polluted location in north India, J. Geophys. Res., 111, D20214, doi: 10.1029/2006JD007142.

Safai, P.D., Kewat, S., Pandithurai, G., Praveen, P.S., Ali, K., Tiwari, S., Rao, P.S.P., Budhawant, K.B., Saha, S.K. and Devara, P.C.S. (2008). Aerosol characteristics during winter fog at Agra, North India. J. Atmos. Chem., 61:101–118.

Sandradewi, J., Prévôt, A. S. H., Weingartner, E., Schmidhauser, R., Gysel, M., Baltensperger, U., (2008a). A study of wood burning and traffic aerosols in an Alpine valley using a multi-wavelength Aethalometer. Atmos. Environ., 42, 101–112.

Sandradewi, J., Prévôt, A. S. H., Szidat, S., Perron, N., Alfarra, M.R., Lanz, V. A., Weingartner, E., Baltensperger, U. (2008b). Using aerosol light absorption measurements for the quantitative determination of wood burning and traffic emission contributions to particulate matter. Environ. Sci. Technol. 42, 3316–3323. Doi: 10.1021/es702253m.

Singh, A. and Dey, S. (2012). Influence of aerosol composition on visibility in megacity Delhi. Atmos. Environ. 62 :367-373.

Srivastava, S.K., Sharma, A.R., Sachdeva, K. (2016). A ground observation based climatology of winter fog: Study over the Indo-Gangetic Plains, India. International Journal of Science, Engineering and Technology, 7, 742-753.

Takemura, T., Nakajima, T., Dubovik, O., Holben, B.N.and Kinne, S. (2002). Single scattering albedo and radiative forcing of various aerosol species with a global three dimensional model. J. Clim., 15, 333–352.

Tiwari, S., Payra, S., Mohan, M., Verma, S. and Bisht, D.S. (2011). Visibility degradation during foggy period due to anthropogenic urban aerosol at Delhi, India. Atmos. Poll. Res. 2, 116-120.

Tripathi, S.N., Tare, V., Chinman, N., Srivastava, A.K., Dey, S. (2006). Measurements of atmospheric parameters during Indian Space Research Organization Geosphere Biosphere Programme Land Campaign II at a typical location in the Ganga basin: 1. Physical and optical properties. J. Geophys. Res., 111, D23209, doi: 10.1029/2006JD007278.

Zhang, R., Khalizov, A.F., Pagels, J., Zhang, D., Xue, H. and McMurry, P.H. (2008). Variability in morphology, hygroscopicity, and optical properties of soot aerosols during atmospheric processing. Proc. Natl. Acad. Sci.U.S.A. 105, 10291–10296.

Zhao, M., Xiu, G., Qiao, T., Li, Y. and Yu, J. (2016). Characteristics of Haze Pollution Episodes and Analysis of a Typical Winter Haze Process in Shanghai. Aerosol Air Quality Res. 16: 1625–1637.

List of Figures:

Fig.1: Variation of daily mean (a) mass concentration of BC, (b) σ_{sca} and σ_{abs} in comparison with the atmospheric visibility ~~at IGIA~~ during WIFEX 2015-16.

Fig.2: Computed visibility (from Koschmieder formula) and RVR measured visibility at IGI Airport, New Delhi during WIFEX 2015-16.

Fig.3: Mean σ_{sca}, σ_{abs}, σ_{ext}, BC mass and SSA during dense foggy and less foggy period during WIFEX 2015-16.

Fig.4: Variation of (a) BC mass, (b) SSA, (c) σ_{abs} and (d) $\sigma_{sca,}$ during dense foggy and less foggy period during WIFEX 2015-16.

Fig.5: Variation of meteorological parameters and DT in comparison with atmospheric visibility during dense fog on 23-24 Jan 2016(Dotted vertical line indicates commencement of dense fog).

Fig.6: Variation of (a) CCN at different suspersaturations and (b) σ_{sca} and σ_{abs} during the dense foggy period on 23-24 Jan 2016.

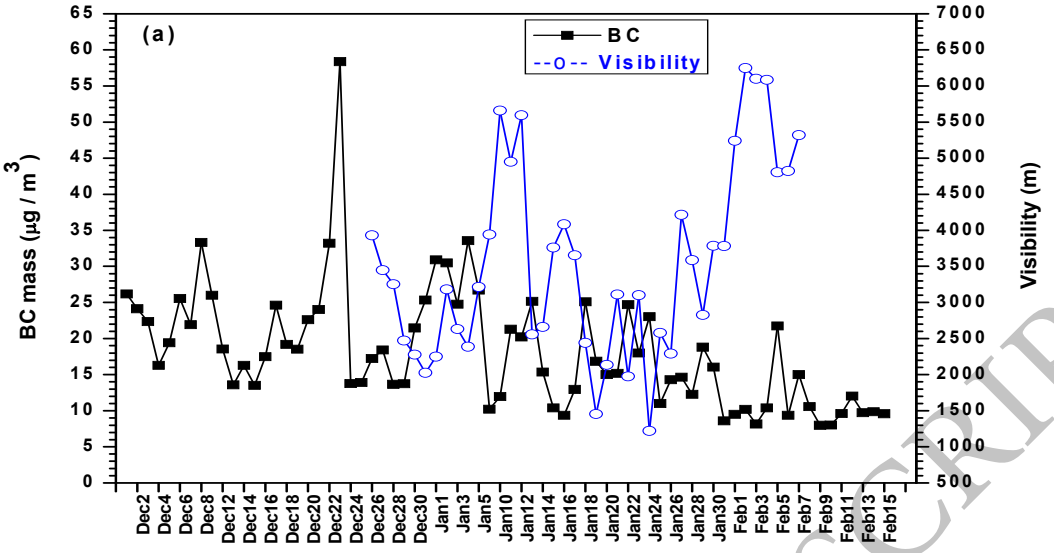

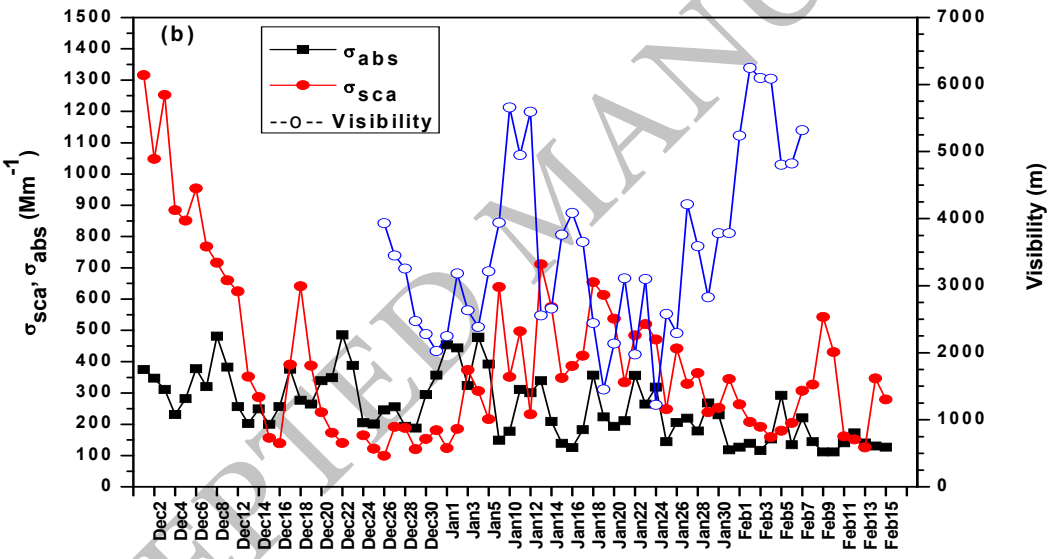

Fig.1: Variation of daily mean (a) mass concentration of BC, (b) σ_{sca} and σ_{abs} in comparison with the atmospheric visibility ~~at IGIA~~ during WIFEX 2015-16.

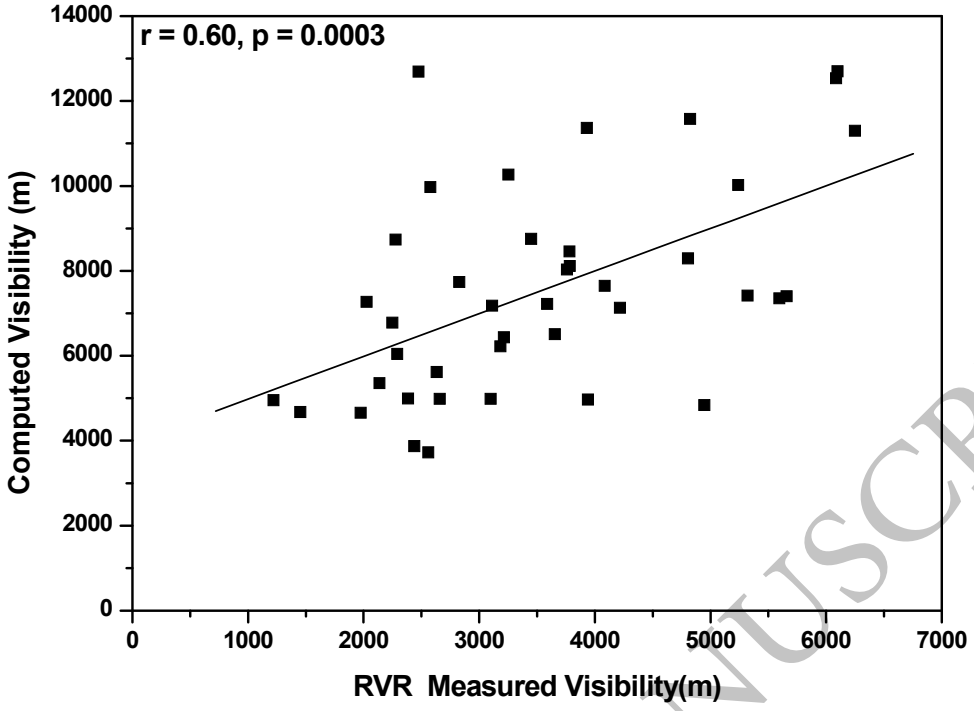

Fig.2: Computed visibility (from Koschmieder formula) and RVR measured visibility at IGI Airport, New Delhi during WIFEX 2015-16.

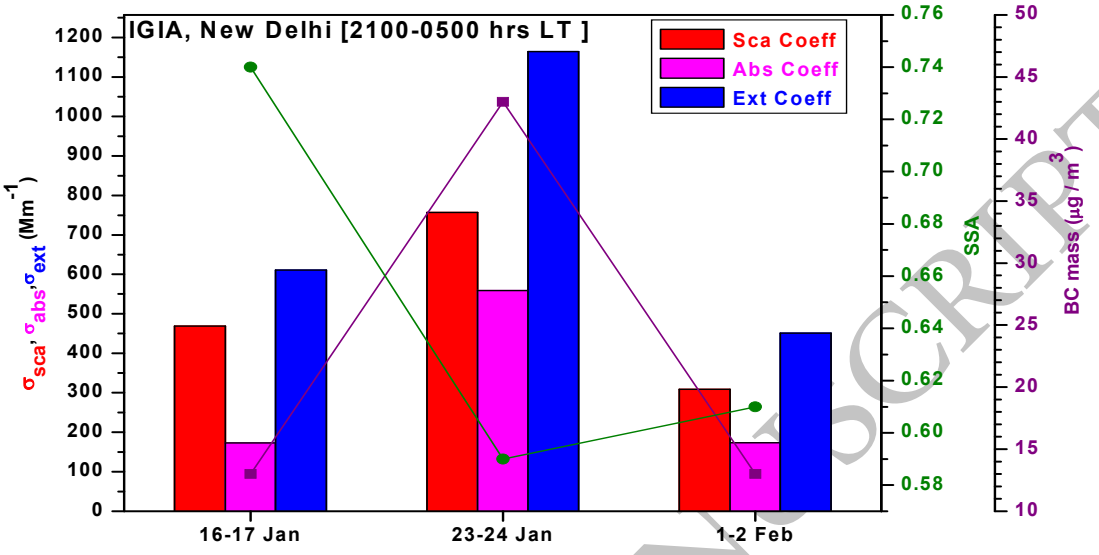

Fig.3: Mean σ_{sca}, σ_{abs}, σ_{ext}, BC mass and SSA during dense foggy and less foggy period during WIFEX 2015-16.

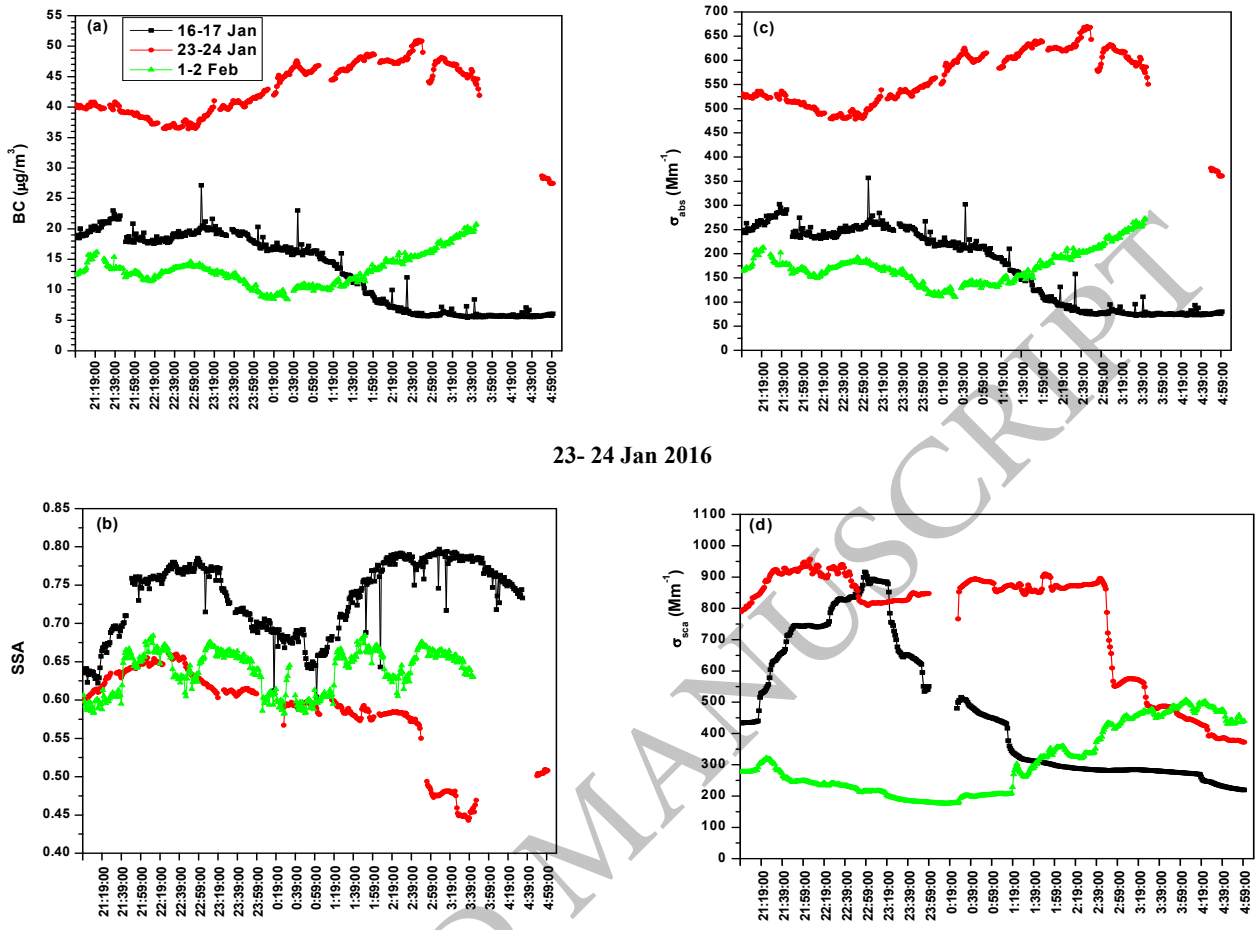

Fig.4: Variation of (a) BC mass, (b) SSA, (c) σ_{abs} and (d) $\sigma_{sca,}$ during dense foggy and less foggy period during WIFEX 2015-16.

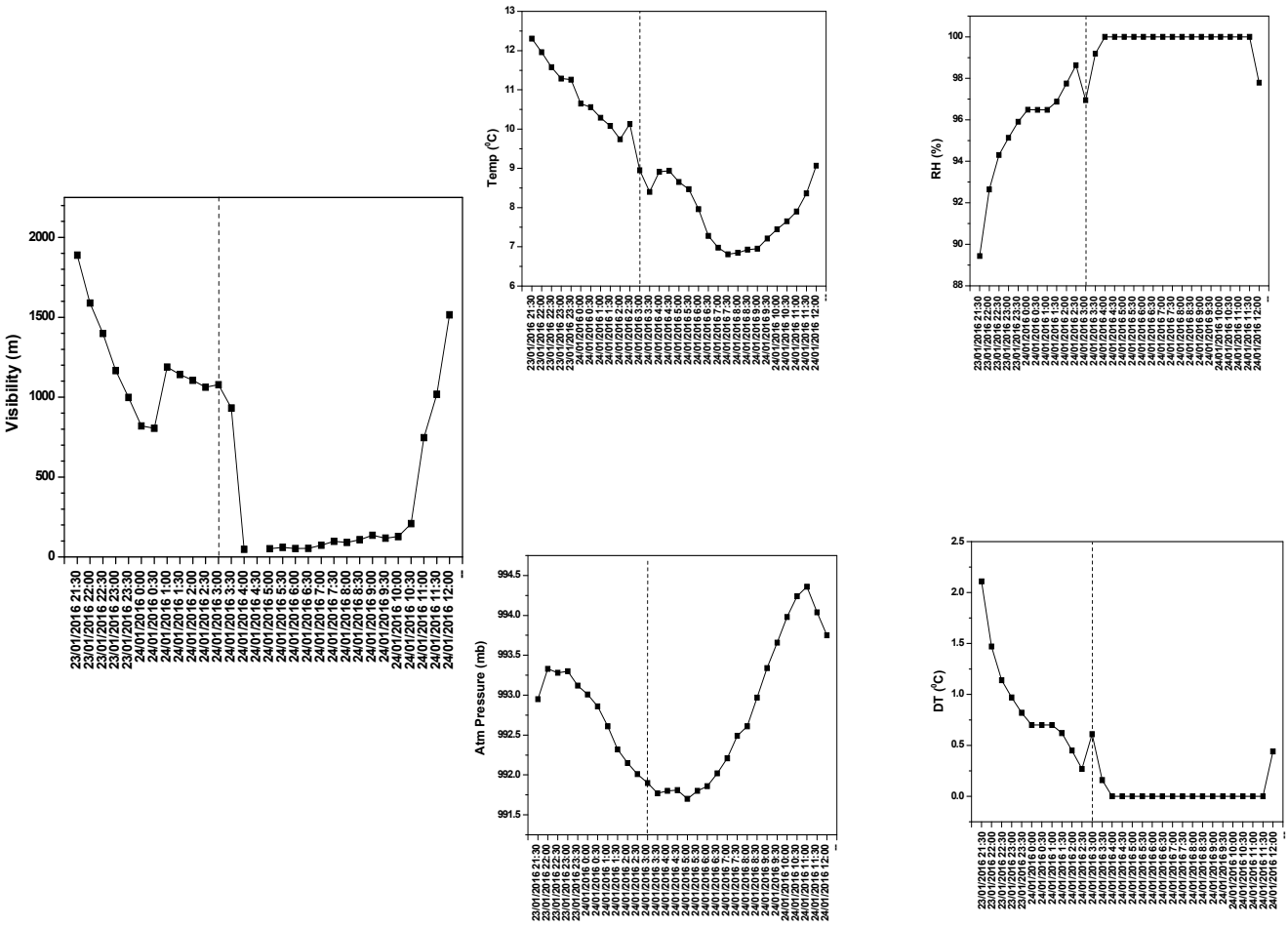

Fig.5: Variation of meteorological parameters and DT in comparison with atmospheric visibility during dense fog on 23-24 Jan 2016 (Dotted vertical line indicates commencement of dense fog).

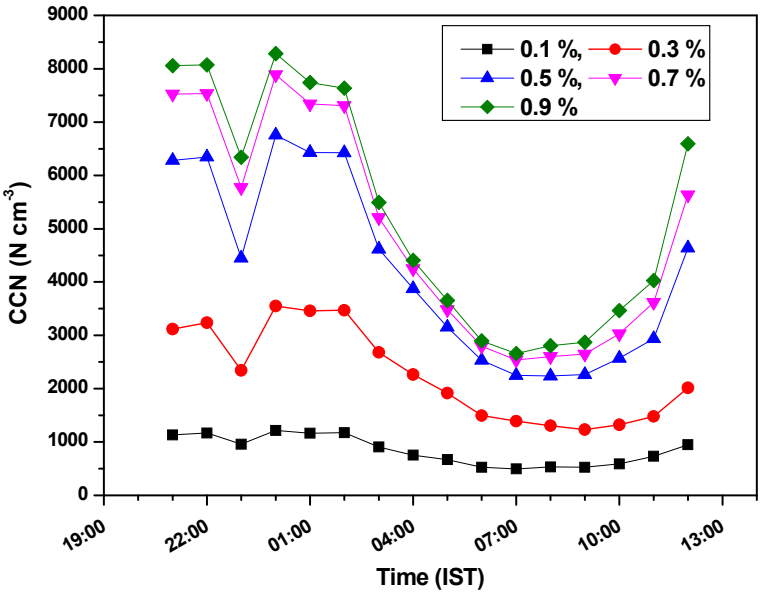

583

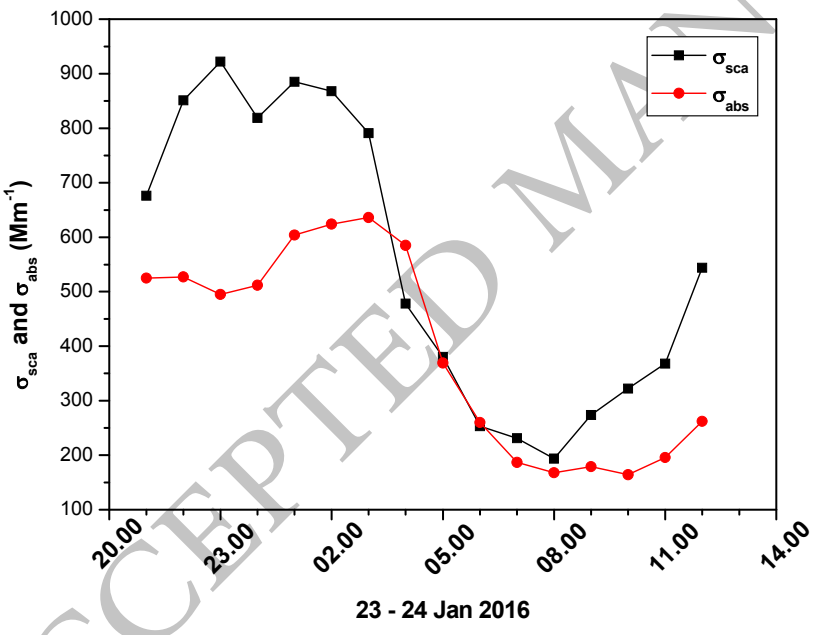

584
585 Fig.6: Variation of (a) CCN at different suspersaturations and (b) σ_{sca} and σ_{abs} during the dense
586 foggy period on 23-24 Jan 2016.
587